

CMBE11

2nd International Conference on Computational & Mathematical Biomedical Engineering

30st March – 1st April, 2011, Swansea University, UK

Edited by:

Perumal Nithiarasu

Civil and Computational Engineering Centre
School of Engineering, Swansea University
Swansea, UK

Rainald Löhner

Center for Computational Fluid Dynamics
College of Sciences, George Mason University
Fairfax, Virginia, US

Raoul van Loon

Civil and Computational Engineering Centre
School of Engineering, Swansea University
Swansea, UK

Igor Sazonov

Civil and Computational Engineering Centre
School of Engineering, Swansea University
Swansea, UK

Xianghua Xie

Department of Computer Science, Swansea University
Swansea, UK

PATIENT-SPECIFIC FINITE ELEMENT ANALYSIS OF CAROTID ARTERY STENTING: IMPACT OF CONSTITUTIVE VESSEL MODELING ON VESSEL WALL STRESS DISTRIBUTION F. Auricchio, M. Conti, A. Ferrara, S. Morganti, A. Reali	367
THE MECHANICAL RESONSE OF THE HUMAN CORONARY ARTERY: SIMULATION BY HIGH ORDER FINITE ELEMENT ANALYSIS E. Priel, Z. Yosibash	371
REGIONAL DIFFERENCES IN MECHANICAL BEHAVIOR OF THE THORACIC AORTA DURING PRESSURE-INDUCED INFLATION J. Kim, S. Baek	375
COMPUTATIONAL STUDY OF BLOOD FLOW WITHIN A MULTI-BRANCHED MODEL OF THE RABBIT THORACIC AORTA A. M. Plata, P. E. Vincent, A. A. E. Hunt, S. J. Sherwin, P. D. Weinberg	379
SWIRLGRAFT VERSUS CONVENTIONAL STRAIGHT GRAFT AS VASCULAR ACCESS: A FULL CFD-ANALYSIS K. Van Canneyt, G. De Santis, S. Eloot, P. Segers, P. Verdonck	383
NUMERICAL MODEL FOR THE CFD-SIMULATION OF THE FLOW FIELD IN THE ANASTOMOSIS REGION OF CORONARY BYPASSES M. De Witte, A. Swillens, L. Løvstakken, H. Nordgaard, D. Van Loo, B. Trachet, J. Vierendeels, P Segers	387
RESULTS OF THE FDA INTERLABORATORY COMPUTATIONAL S.F.C. Stewart, P. Hariharan, E.G. Paterson, G.W. Burgreen, V. Reddy , S.W. Day, M. Giarra, K.B. Manning, S. Deutsch, M.R. Myers, M.R. Berman, R.A. Malinauskas	391
VESSEL WALL MODELING FOR 1D HAEMODYNAMICS S.S. Simakov, Y.V. Vassilevski, V.Yu. Salamatova, Y.A. Ivanovy, T.K. Dobroserdova	395

SS-5: Surgical Simulation

A COMPUTATIONAL FRAMEWORK FOR UNCERTAINTY QUANTIFICATION AND ROBUST OPTIMIZATION OF CARDIOVASCULAR BYPASS GRAFT SURGERIES. Sankaran, A.L. Marsden	399
APPLICATION OF GENETIC ALGORITHM AND FINITE ELEMENT METHOD IN DESIGN OF THE SCAFFOLDS FOR TISSUE ENGINEERING M.K. Heljak, W. Swieszkowski K.J. Kurzydowski	403
MODELLING VENTRICULAR FUNCTION UNDER LVAD SUPPORT M. McCormick, D. Nordsletten, D. Kay, N. Smith	407

NUMERICAL MODEL FOR CFD-SIMULATION OF THE FLOW FIELD IN THE ANASTOMOSIS REGION OF CORONARY BYPASSES

Marloes De Witte*, Abigail Swillens*, Lasse Løvstakken, Håvard Nordgaard**,
Denis Van Loo***, Bram Trachet*, Jan Vierendeels**** and Patrick Segers***

* IBiTech-bioMMeda, Ghent University, Ghent, Belgium

** Department of Circulation and Medical Imaging, Norwegian University of Science
and Technology, Trondheim, Norway

***Department of Physics and Astronomy (UGCT), Department of Soil Management,
Ghent University, Ghent, Belgium

**** Department of Flow, Heat and Combustion Mechanics, Ghent University, Ghent,
Belgium

Corresponding author: Marloes De Witte, Ph. D. fellow of the Research Foundation -
Flanders (FWO), IBiTech-bioMMeda, Ghent University, De Pintelaan 185 Blok B, B-
9000 Gent, Belgium, Marloes.DeWitte@UGent.be

SUMMARY

Coronary artery bypass surgery is a treatment for ischemic heart disease and can increase life quality and expectancy. The results after the treatment depend largely on the patency of the bypass grafts, which are used to bypass the narrowed arteries on the heart. Long-term patency is mainly determined by the progression of atherosclerosis and intimal hyperplasia (IH) within the bypass grafts, which are believed to be related to unfavourable wall shear stress (e.g. low and oscillatory WSS) exerted on the endothelial cells. To investigate the potential role of hemodynamic forces on the endothelial cells and the impact of the severity of the bypassed arterial stenosis on the flow fields, we developed a computational model of a LIMA-to-LAD anastomosis region obtained from a porcine in-vivo cast. In addition, the same porcine experiment provided the necessary up- and downstream boundary conditions for the simulations. The model has been applied to simulate the flow field in 5 cases, corresponding with 100, 97, 90, 75 and 0% LAD stenosis, in order to quantify the effect of the stenosis on resulting flow fields and on WSS distributions. Low stenosis degrees are associated with competitive LAD and LIMA flow and low WSS in the LIMA, which might contribute to WSS-related remodeling and suboptimal performance of the LIMA bypass.

Key Words: *LIM-to-LAD anastomosis, numerical modeling, CFD, wall shear stress.*

1. INTRODUCTION

Atherosclerosis may lead to flow-obstructing stenosis, a problem that frequently occurs in the coronary arteries and causes angina pectoris and heart infarction. In order to restore the blood supply to the heart, the atherosclerotic coronary arteries can be bypassed by means of a vascular graft. This treatment is called coronary artery bypass surgery. Different kinds of vessels may be used as bypass graft (vein or artery). In this work, the LIMA graft and LIMA-to-LAD anastomosis are studied (host: left anterior descending coronary artery, LAD; graft: left internal mammary artery, LIMA).

Despite the usually excellent long-term patency of the LIMA-graft, the LIMA-graft may shrivel and fail in the late course after the grafting procedure. This so-called ‘string effect’, is more likely to occur in conditions of competitive flow, where the native flow is substantial and disturbs the flow through the bypass grafts due to a non-significant stenosis [1].

It is known that hemodynamic forces, principally too low ($WSS < \pm 0.4\text{--}0.5\text{Pa}$) and oscillatory WSS, may induce endothelial dysfunction and vascular remodeling and promote atherosclerosis and IH [2, 3]. In order to assess the susceptibility of the LIMA-graft to narrowing and shriveling, more insight has to be acquired in the complex flow field and the induced WSS in the LIMA-lumen. As WSS is still a challenging parameter to measure non-invasively, numerical simulations are necessary.

2. MAIN BODY

2.1 Materials and Methods

2.1.1 3D-geometry

A LIMA-to-LAD bypass was constructed in a pig [4]. During the procedure, flow and pressure measurements were performed in the proximal and distal LAD, and flow was measured in the LIMA. Three data sets were acquired, measured when the proximal LAD was completely occluded, partially occluded and fully open. Afterwards, the heart was removed from the euthanized pig's chest and the LIMA was fixated on the heart in order to preserve the angle between LAD and LIMA. Subsequently, a cast was made of the anastomosis region (with non-occluded LAD). This 3D-cast of the anastomosis region and surrounding vasculature was scanned using the micro-CT scanner of the Ghent University Centre for X-ray Tomography. Out of the resulting CT-images, a digital model (STL) was created using Mimics (Materialise, Belgium). The resulting basic model counted 2 circular inlets (LIMA and proximal LAD), and 13 circular outlets (12 septals and the distal LAD).

As the exact degree of stenosis was not known, (digital) models with proximal LAD stenoses of 97, 90 and 75% area reduction were created by extending the proximal LAD inlets of three basic models by means of three cylindrical tubes of which the mid luminal flow sections were reduced by respectively 97, 90 and 75% (figures 3B, C and D). The models for 0% and 100% stenosis were obtained by defining the proximal LAD inlet respectively as an inlet and as a wall (figures 3A and E). Finally, the resulting geometries were meshed in Gambit (Ansys, Inc., U.S.A.).

2.1.2 Boundary conditions

In order to identify the isolated effects of the stenoses as purely as possible, *one* set of boundary conditions (BC's) was used to simulate flow in the 5 different configurations. The BC's were extracted from the data measured during 100% LAD occlusion as this condition provided the most consistent and useful dataset.

The pressure measured at the proximal LAD was applied at both inlets (LIMA and proximal LAD) because no LIMA-pressure measurements were available. This induces an error since a time shift between both pressure waves is expected in real physiologic circumstances.

Since flow in the coronary circulation is dominated by active components during systole (e.g. the squeezing of the septals embedded in the myocardium) and more by passive components during diastole, two types of boundary conditions were created for systole and diastole. During the whole cardiac cycle, velocity profiles were assumed parabolic at the outlets.

As the exact distribution of blood flow towards the distal LAD and the septals is unknown, we arbitrarily assumed that 5% of the blood flow was going to the septals, while the remaining 95% was going to the distal LAD. During systole, the maximal velocity of the parabolic velocity profile at septal l ($l=1\text{--}12$) was then calculated according to:

$$v_{systole}^{l,max}(t) = -2 \times \left[\frac{0.05 \times Q_{LIMA}(t)}{A_l} \left(\frac{R_l^3}{\sum_{k=1}^{12} R_k^3} \right) \right]$$

with A_l and R_l respectively the area and radius of the circular outflow section of septal l and $Q_{LIMA}(t)$ the flow measured at the LIMA at time instant t during 100% proximal LAD occlusion. The maximal velocity of the parabolic velocity profile at the distal LAD was calculated according to:

$$v_{systole}^{LAD,max}(t) = -2 \times \left[\frac{0.95 \times Q_{LIMA}(t)}{A_{LAD}} \right]$$

During diastole, the maximal velocities of the parabolic outlet velocity profiles at septal l and at the distal LAD at a time t were calculated by means of the conductances $C_l(t)$ and $C_{LAD}(t)$, given by respectively:

$$C_l(t) = \frac{0.05 \times Q_{LIMA}(t)}{P_{LIMA}(t) - P_{ra}} \left(\frac{R_l^3}{\sum_{k=1}^{12} R_k^3} \right) \quad \text{and} \quad C_{LAD}(t) = \frac{0.95 \times Q_{LIMA}(t)}{P_{LIMA}(t) - P_{ra}}$$

with $P_{LIMA}(t)$ the pressure applied at the LIMA (i.e., the pressure measured at the proximal LAD during 100% proximal LAD occlusion) and $P_{ra} \approx 0$ the pressure in the right atrium.

The obtained conductances (calculated from the measurements corresponding with 100% proximal LAD occlusion) were used to derive the maximal velocities of the parabolic velocity profiles at septal l and at the distal LAD according to:

$$v_{diastole}^{l/LAD,max}(t) = -2 \times \left[C_{l/LAD}(t) \frac{P_{l/LAD}(t)}{A_{l/LAD}} \right]$$

with $P_{l/LAD}(t)$ the pressure at septal l or at the distal LAD. Velocities are thus dependent on the local pressures in the studied models.

During diastole, a semi-implicit calculation of the flow field is necessary since $P_{l/LAD}(t)$, a result of the flow simulations, must be known in order to calculate the corresponding outflow profile. An adapted algorithm was developed to accomplish this.

All simulations were performed using Fluent 12 (Ansys, Inc., U.S.A.). Two cardiac cycles were calculated to remove transient effects.

2.2 Results and Discussion

2.2.1 Effect of the stenosis on the flow and flow patterns

The total blood flow into the anastomosis region is not affected by the degree of proximal LAD stenosis. Lower flow from the LAD causes higher flow from the LIMA, and vice versa. However, the lower the degree of proximal LAD stenosis, the higher the inflow into the proximal LAD and the lower the inflow of blood into the LIMA, as illustrated in figure 1.

In all studied cases, the velocity contours at maximal inflow in slices distal from the anastomosis-region, show typical crescent velocity distributions with maximal velocities near the bottom wall of the LAD (figure 2A, slices 6-9). The angle between LIMA and LAD affects the velocity distribution in the anastomosis region: e.g. in slice 8 of figure 2A, velocities are higher near the back wall of the LAD due to the twisted position of the LIMA relatively to the LAD (figure 2B, top view of the LIMA-to-LAD anastomosis).

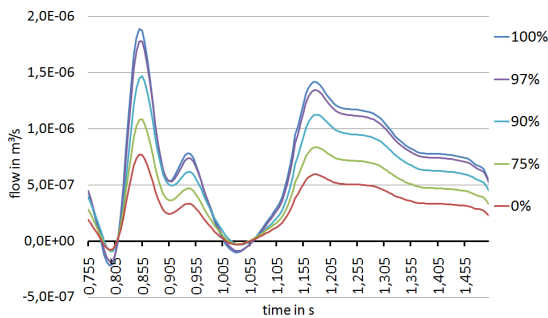


Figure 1: Plot of the flow at the LIMA (inlet) for 100, 97, 90, 75 and 0% LAD stenosis

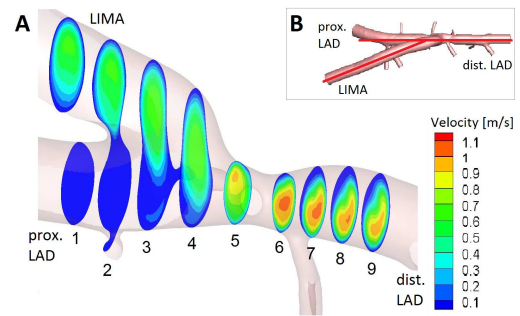


Figure 2: (A) Velocity contours in 9 cross-sectional planes at $t=0.855s$ for 100% prox. LAD occlusion; (B) Top view of the LIMA-to-LAD anastomosis

2.2.2 Effect of the stenosis on the WSS-distribution

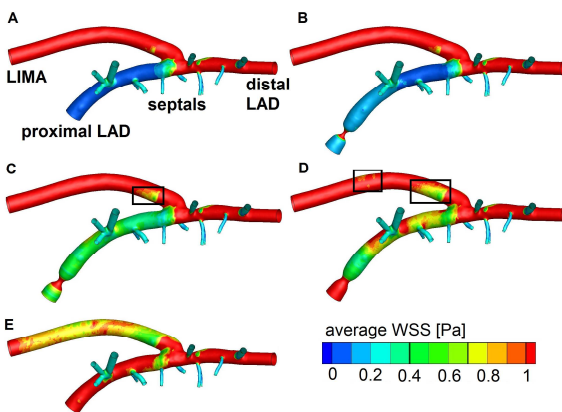


Figure 3: Average WSS (0-1Pa; $WSS > 1Pa$ = red) during one cardiac cycle for the cases of (A) 100%, (B) 97%, (C) 90%, (D) 75% and (E) 0% proximal LAD occlusion

The average WSS in the LIMA (whole cardiac cycle) is clearly correlated to the blood flow through it: for a proximal LAD occlusion of 100 or 97%, the average WSS in the LIMA is higher than 1Pa (figures 3A and B); when the flow in the LIMA diminishes (90% stenosis), a zone of relatively low average WSS (0.3-0.8Pa) appears at the inner bend of the distal LIMA, as indicated in figure 3C. This zone of low average WSS expands when the degree of proximal LAD stenosis is further lowered (i.e. in the case of 75% stenosis, figure 3D) until it covers the whole LIMA when the proximal LAD is not occluded (figure 3E).

3. CONCLUSIONS

In conclusion, based on hemodynamic grounds, the LIMA may become more susceptible for vascular diseases and subsequent occlusion when the stenosis in the proximal LAD is less than severe.

REFERENCES

- [1] M.B. Yilmaz, Y. Guray et al., Fate of internal mammary artery grafted to left anterior descending artery is influenced by native vessel stenosis and viable myocardium, *Angiology*, Vol. 60, Issue 2, 201-206, 2009.
- [2] A.M. Malek, S.L. Alper and S. Izumo, Hemodynamic shear stress and its role in atherosclerosis, *JAMA*, Vol. 282, No. 21, 2035-2042, 1999.
- [3] G.S. Kassab and J. Navia, Biomechanical considerations in the design of graft: the homeostasis hypothesis, *Annual Review of Biomedical Engineering*, Vol. 8, 499-535, 2006.
- [4] H. Nordgaard, D. Nordhaug et al., Different graft flow patterns due to competitive flow or stenosis in the coronary anastomosis assessed by transit-time flowmetry in a porcine model, *European Journal of Cardio-Thoracic Surgery*, Vol. 6, Issue 1, 137-142, 2009